

RESEARCH ARTICLE

Effectiveness Factors and Conversion in a Biocatalytic Membrane Reactor

Buntu Godongwana*

Department of Chemical Engineering, Cape Peninsula University of Technology, Cape Town, South Africa

* godongwanab@cput.ac.za



OPEN ACCESS

Citation: Godongwana B (2016) Effectiveness Factors and Conversion in a Biocatalytic Membrane Reactor. PLoS ONE 11(4): e0153000. doi:10.1371/journal.pone.0153000

Editor: Bing Xu, Brandeis University, UNITED STATES

Received: January 5, 2016

Accepted: March 22, 2016

Published: April 22, 2016

Copyright: © 2016 Buntu Godongwana. This is an open access article distributed under the terms of the [Creative Commons Attribution License](https://creativecommons.org/licenses/by/4.0/), which permits unrestricted use, distribution, and reproduction in any medium, provided the original author and source are credited.

Data Availability Statement: All relevant data are within the paper.

Funding: The study was funded by the National Research Foundation of South Africa (<http://www.nrf.ac.za/>), grant number 87845. The funders had no role in study design, data collection and analysis, decision to publish, or preparation of the manuscript.

Competing Interests: The authors have declared that no competing interests exist.

Abbreviations: B_m , constants of integration of Bessel's equation, $m = 1, 2$; c , substrate concentration (g dm^{-3}); c_b , bulk lumen concentration (g dm^{-3}); c_0 , substrate feed concentration (g dm^{-3});

Abstract

Analytical expressions of the effectiveness factor of a biocatalytic membrane reactor, and its asymptote as the Thiele modulus becomes large, are presented. The evaluation of the effectiveness factor is based on the solution of the governing equations for solute transport in the two regions of the reactor, i.e. the lumen and the matrix (with the biofilm immobilized in the matrix). The lumen solution accounts for both axial diffusion and radial convective flow, while the matrix solution is based on Robin-type boundary conditions. The effectiveness factor is shown to be a function of the Thiele modulus, the partition coefficient, the Sherwood number, the Peclet number, and membrane thickness. Three regions of Thiele moduli are defined in the effectiveness factor graphs. These correspond with reaction rate limited, internal-diffusion limited, and external mass transfer limited solute transport. Radial convective flows were shown to only improve the effectiveness factor in the region of internal diffusion limitation. The assumption of first order kinetics is shown to be applicable only in the Thiele modulus regions of internal and external mass transfer limitation. An iteration scheme is also presented for estimating the effectiveness factor when the solute fractional conversion is known. The model is validated with experimental data from a membrane gradient reactor immobilised with *Phanerochaete chrysosporium* for the production of lignin and manganese peroxidases. The developed model and experimental data allow for the determination of the Thiele modulus at which the effectiveness factor and fractional conversion are optimal.

Introduction

Membrane bioreactors (MBR's) offer a number of advantages over traditional bioreactors and their use for various bioconversions have been extensively reported [1–3]. The main challenge in the use of MBR's remains the diffusional resistance of the membrane which adversely affects their performance [4,5]. The effectiveness factor (η), defined as the ratio of the observed rate of reaction to the hypothetical rate in the absence of mass transfer limitations [6], is generally used to evaluate the performance of a catalytic reactor. A thorough review of mathematical methods employed in evaluating exact solutions of this parameter was given by Aris [6]. This study presented effectiveness factors for single and multiple reactions taking place in various

$C = c/c_0$, dimensionless substrate concentration; D_{AB} , substrate diffusivity ($m^2 s^{-1}$); $f = u_1/u_0$, fraction retentate; $J_n(\lambda)$, Bessel function of order n of the first kind; k_a , mass transfer coefficient ($m s^{-1}$); k_m , membrane hydraulic permeability ($m Pa^{-1} s^{-1}$); K_m , saturation (or Monod constant) ($g dm^{-3}$); $k_m^* = k_m/c_0$, dimensionless Monod constant; L , membrane effective length (m); $M(a,b,\theta)$, Kummer function of the first kind; $Pe_u = u_0 R_1 / D_{AB}$, axial Peclet number; $Pe_v = v_0 R_1 / D_{AB}$, radial Peclet number; r , radial spatial coordinate (m); $R = r/R_1$, dimensionless radial spatial coordinate; R_1 , membrane lumen radius (m); $Re = \rho u_0 R_1 / \mu$, Reynolds number; $Sc = \mu / \rho D_{AB}$, Schmidt number; $Sh = k_a R_1 / D_{AB}$, Sherwood number; u , axial velocity ($m s^{-1}$); u_0 , feed axial velocity ($m s^{-1}$); $U = u/u_0$, dimensionless axial velocity; v , radial velocity ($m s^{-1}$); $v_0 = k_m(\rho_0 - \rho_s)$, permeation velocity ($m s^{-1}$); $V = v/v_0$, dimensionless radial velocity; V_m , maximum rate of reaction ($g dm^{-3} s^{-1}$); X , average biofilm density ($g dm^{-3}$); $Y_{x/s}$, yield of biofilm per unit substrate; z , axial spatial coordinate (m); $Z = z/L$, dimensionless axial spatial coordinate; β , dimensionless transmembrane pressure; γ , membrane partition coefficient; $\delta = K_m/c_0 C_b$, modified dimensionless Monod constant; $\epsilon = 1/\phi$, substitution variable; η , effectiveness factor for general kinetics; η_0 , effectiveness factor for zero-order kinetics; η_1 , effectiveness factor for first-order kinetics; θ , substitution variable; $\kappa = \mu k_m L / R_1^2$, dimensionless membrane hydraulic permeability; λ_m , eigen values, $m = 1, 2, \dots$; μ , solution dynamic viscosity ($Pa s$); μ_{max} , maximum specific growth rate (s^{-1}); ρ , solution density ($kg m^{-3}$); $\phi = R_1/L$, aspect ratio; ϕ , Thiele modulus; ψ , external resistance to mass transfer; Y , fractional conversion.

shapes of porous catalysts. Webster and co-workers [7,8] presented analytical models for a membrane bioreactor immobilized with whole cells, based on both Robin-type and Dirichlet-type boundary conditions. The former boundary type accounts for external mass transfer limitations, while the latter assumes the concentration at the membrane wall is known. Willaert *et al.* [9] obtained identical effectiveness factor expressions to Webster and Shuler [7] based on Dirichlet boundary conditions. In these studies, as well as in the majority of available exact solutions [10–12], axial diffusion and radial convective flows are neglected and the kinetics are generally considered linear. These assumptions are not always justified [13] and are imposed with the intention of attaining closed-form expression of the transport equation. The analytical solution of the mass balance equation is not always feasible, and a number of numerical schemes have been developed for this purpose [14–20]. Analytical models however are preferred for their simplicity.

The current analysis is aimed at developing expressions of the effectiveness factor for an MBR immobilized with biofilm, based on the model developed by Godongwana *et al.* [13]. The asymptotic behaviour as the Thiele-modulus becomes large will be considered. The models are based on the MBR system shown in Fig 1, and the following conditions of operation are assumed: (1) the system is isothermal; (2) the flow regime within the membrane lumen is fully developed, laminar, and homogeneous; (3) the physical and transport parameters are constant; (4) in the membrane matrix the flow is only one dimensional (i.e. there are no axial components of the velocity in the membrane matrix).

Mathematical Formulation

Governing equations

The governing equations for solute transport in the lumen and matrix of the MBR are respectively:

$$u_1 \frac{\partial c_1}{\partial z} + v_1 \frac{\partial c_1}{\partial r} = D_1 \left[\frac{1}{r} \frac{\partial}{\partial r} \left(r \frac{\partial c_1}{\partial r} \right) + \frac{\partial^2 c_1}{\partial z^2} \right] \tag{1}$$

$$\frac{D_2}{r} \frac{\partial}{\partial r} \left(r \frac{\partial c_2}{\partial r} \right) - v_2 \frac{\partial c_2}{\partial r} = \frac{V_m c_2}{K_m + c_2} \tag{2}$$

The MBR is considered axisymmetric and the associated boundary conditions to Eqs (1) and (2) are:

$$B.C.1 \text{ at } z = 0 \quad \forall r \quad c_1 = c_0 \tag{3a}$$

$$B.C.2 \text{ at } r = 0 \quad \forall z \quad \frac{\partial c_1}{\partial r} = 0 \tag{3b}$$

$$B.C.3 \text{ at } r = R_1 \quad \forall z \quad \frac{\partial c_1}{\partial z} = \frac{2D_1}{u_1 R_1} \frac{\partial c_1}{\partial r} \tag{3c}$$

$$B.C.4 \text{ at } r = R_1 \quad \forall z \quad k_a(c_{1b} - c_{1E}) = -D_2 \frac{\partial c_2}{\partial r} \tag{3d}$$

$$B.C.5 \text{ at } r = R_2 \quad \forall z \quad \frac{\partial c_2}{\partial r} = 0 \tag{3e}$$

where u and v are the axial and radial velocity components, respectively; c_1 and c_2 are the local

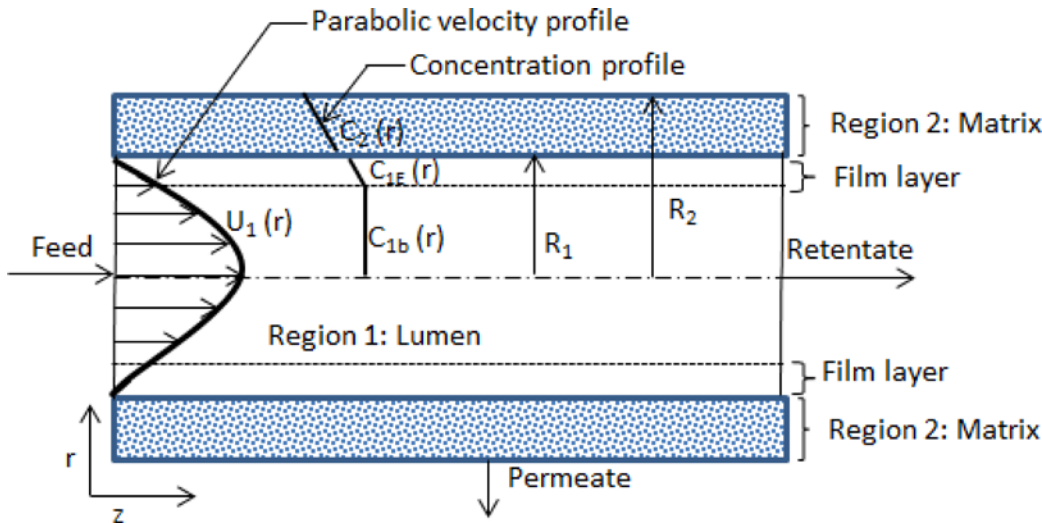


Fig 1. A cross-section of the membrane bioreactor illustrating the different regions of the MBR (i.e. lumen, film layer, and matrix). The velocity distribution and concentration distribution are also shown.

doi:10.1371/journal.pone.0153000.g001

substrate concentrations in the lumen and fiber matrix, respectively; c_{1b} is the bulk lumen concentration; c_{1E} is the concentration on the internal surface of the membrane; D_1 and D_2 are the substrate diffusion coefficients in the lumen and matrix, respectively; k_a is the mass transfer coefficient; K_m is the saturation constant; and V_M is the maximum rate of reaction.

Boundary condition 1 (B.C.1) corresponds to a uniform inlet substrate concentration; B.C.2 corresponds to cylindrical symmetry at the centre of the membrane lumen; B.C.3 and B.C.4 corresponds to continuity of the substrate flux at the lumen-matrix interface. The partition coefficient for the transfer from outside the film layer to inside the film is assumed to be unity. Only the partition for the transfer from the film layer to the matrix is considered, as shown in Fig 1. B.C.5 implies there is no diffusion across the matrix-shell interface. In single-substrate limited biofilms, V_M in Eq (2) is given by [21]:

$$V_M = \frac{\mu_{max}X}{Y_{X/S}} \tag{4}$$

where X is the average biofilm density, μ_{max} is the maximum specific growth rate, and $Y_{X/S}$ is the yield of biofilm per unit substrate.

MBR lumen (Region 1)

In the lumen-side of the MBR, Eq (1) in dimensionless form becomes:

$$\phi Pe_u U_1 \frac{\partial C_1}{\partial Z} - \phi^2 \frac{\partial^2 C_1}{\partial Z^2} = \frac{1}{R} \left(\frac{\partial C_1}{\partial R} + R \frac{\partial^2 C_1}{\partial R^2} \right) - Pe_v V_1 \frac{\partial C_1}{\partial R} \tag{5}$$

where:

$$U = \frac{u}{u_0}; V = \frac{v}{v_0}; C = \frac{c}{c_0}; Z = \frac{z}{L}; R = \frac{r}{R_1}; \phi = \frac{R_1}{L}$$

$$Pe_u = \frac{u_0 R_1}{D_1}; Pe_v = \frac{v_0 R_1}{D_1} \tag{6}$$

The solution of Eq (5) was given by Godongwana *et al.* [13] as an asymptotic expansion in terms of the membrane hydraulic permeability κ :

$$C_1(\theta, x) = \sum_{m=1}^{\infty} \sum_{n=0}^N B_m F_m(\theta) T_n(x) \kappa^n \tag{7}$$

Where

$$\theta = -\left(\frac{\varphi^2}{4Pe_u \kappa \beta}\right) \xi^2; \quad \xi = -\frac{2Pe_u \kappa \beta}{\varphi^2} \left[\frac{1}{(f-1)} + Z\right]; \quad \text{and } x = \lambda_m R \tag{8}$$

and $F_m(\theta)$ in Eq (7) is the Kummer function:

$$F_m(\theta) = M\left(-\frac{\lambda_m^2}{4Pe_u \kappa \beta}, \frac{1}{2}, \theta\right) \tag{9}$$

The zero-order and first-order approximations of $T_n(x)$ in Eq (7) are, respectively:

$$T_0(x) = J_0(x) \tag{10}$$

and

$$T_1(x) = \sigma_1 \left[\frac{(x)^2 J_2(x)}{3!!} + \sigma_2 \frac{(x)^3 J_3(x)}{5!!} + \sigma_3 \frac{(x)^4 J_4(x)}{7!!}\right] \tag{11}$$

where λ_m are the eigenvalues, J_n is the Bessel function of the first kind of order n .

$$\sigma_1 = -\frac{3Pe_v \beta \left(\frac{u_0}{v_0}\right)}{2\lambda_m^2}, \quad \sigma_2 = -\frac{20}{3\lambda_m^2}, \quad \text{and } \sigma_3 = \frac{35}{4\lambda_m^2} \tag{12}$$

The eigenvalues are obtained from B.C.3 in Eq (3c), and are roots of the equation [20]:

$$\frac{\lambda_m \varphi \xi}{\kappa \beta} M\left(-\frac{\lambda_m^2}{4Pe_u \kappa \beta} + 1, \frac{3}{2}, \theta\right) = 4 \frac{J_1(\lambda_m)}{J_0(\lambda_m)} M\left(\frac{-\lambda_m^2}{4Pe_u \kappa \beta}, \frac{1}{2}, \theta\right) \tag{13}$$

The coefficient B_m is obtained by imposing the inlet condition B.C.1 of Eq (3a):

$$B_m = \frac{2}{\lambda_m M\left(-\frac{\lambda_m^2}{4Pe_u \kappa \beta}, \frac{1}{2}, \theta_0\right)} \left[\frac{J_1(\lambda_m)}{J_0^2(\lambda_m) + J_1^2(\lambda_m)}\right] \tag{14}$$

MBR Matrix (Region 2)

First-order Kinetics. The rate of solute consumption inside the membrane matrix is governed by Monod kinetics. Assuming the first-order limit, i.e. $K_m \gg c$, Eq (2) for the matrix in dimensionless form becomes:

$$\frac{d^2 C_2}{dR^2} + \left(\frac{1}{R} - Pe_v V_2\right) \frac{dC_2}{dR} - \phi^2 C_2 = 0 \tag{15}$$

where the first-order Thiele modulus ϕ is defined as:

$$\phi = \sqrt{\frac{V_M R_1^2}{K_m D_2}} \tag{16}$$

Eq (15) is amenable to an analytical solution by regular perturbation only when the hydraulic permeability is much smaller than unity $\kappa \ll 1$. For brevity only the zero-order approximation will be considered, the first order perturbation approximation is given in Appendix A following the procedure of Godongwana *et al.* [13]. Eq (15) then reduces to:

$$\frac{d^2 C_2}{dR^2} + \frac{1}{R} \frac{dC_2}{dR} - \phi^2 C_2 = 0 \tag{17}$$

Eq (17) is evaluated subject to B.C.4, which in dimensionless form becomes:

$$Sh \left(C_b - c_2 / \gamma \right) = - \frac{dC_2}{dR} \Big|_{R=1} \tag{18}$$

Where γ is the partition coefficient and Sh is the Sherwood number. A good estimate of Sh for hollow fiber membranes is given by Wickramasinghe *et al.* [22]:

$$Sh = 1.11 Re^{0.47} Sc^{0.33} \tag{19}$$

where $Sc = \mu / \rho D_{AB}$ is the Schmidt number and $Re = \rho v R_1 / \mu$ is the Reynolds number. The dimensionless bulk lumen concentration is defined as:

$$C_b = 2 \int_0^1 C_1(\theta, x) R dR = 2 \sum_{m=1}^{\infty} \frac{B_m}{\lambda_m} \cdot M \left(-\frac{\lambda_m^2}{4Pe_u \kappa \beta}, \frac{1}{2}, \theta_1 \right) \cdot J_1(\lambda_m) \tag{20}$$

Eq (17) is the modified Bessel's equation and has a solution of the form [23]:

$$C_2 = B_1 I_0(\phi R) + B_2 K_0(\phi R) \tag{21}$$

where I_0 and K_0 are the modified Bessel functions of the first kind and second kind, respectively. The constants B_1 and B_2 are obtained with the use of B.C.4 and B.C.5 as:

$$B_1 = \frac{K_1(\phi R_2) \cdot \gamma C_b}{[K_0(\phi) \cdot I_1(\phi R_2) + I_0(\phi) \cdot K_1(\phi R_2)] + \psi} \tag{22}$$

and

$$B_2 = \frac{I_1(\phi R_2) \cdot \gamma C_b}{[K_0(\phi) \cdot I_1(\phi R_2) + I_0(\phi) \cdot K_1(\phi R_2)] + \psi} \tag{23}$$

where

$$\psi = \frac{\gamma \phi}{Sh} [K_1(\phi) \cdot I_1(\phi R_2) + I_1(\phi) \cdot K_1(\phi R_2)] \tag{24}$$

The effectiveness factor is defined as:

$$\eta = \frac{-2\pi R_1 L D_2 \frac{\partial c_2}{\partial r} \Big|_{r=R_1}}{\pi L (R_2^2 - R_1^2) \frac{V_M c_b}{K_m + c_b}} \tag{25}$$

In dimensionless form:

$$\eta = \frac{-2(\delta + 1)}{\phi_0^2(R_2^2 - 1)} \frac{\partial C_2}{\partial R} \Big|_{R=1} \tag{26}$$

where $\delta = \frac{K_m^*}{C_b}$ and ϕ_0 is the zero-order Thiele modulus defined as:

$$\phi_0 = \sqrt{\frac{V_M R_1^2}{c_0 D_2}} \tag{27}$$

Assuming first-order kinetics ($\delta \gg 1$) Eq (26) reduces to:

$$\eta_1 = \frac{-2}{\phi^2(R_2^2 - 1)C_b} \frac{\partial C_2}{\partial R} \Big|_{R=1} \tag{28}$$

Substituting Eqs (20–24) into Eq (28) gives:

$$\eta_1 = \frac{2\gamma[K_1(\phi) \cdot I_1(\phi R_2) - I_1(\phi) \cdot K_1(\phi R_2)]}{\phi(R_2^2 - 1)\{[K_0(\phi) \cdot I_1(\phi R_2) + I_0(\phi) \cdot K_1(\phi R_2)] + \psi\}} \tag{29}$$

The reciprocal of the effectiveness factor is generally considered a mass transfer resistance [6,8,24]. Thus, the reciprocal of Eq (29) is the sum of the internal resistance and the external resistance (ψ) to mass transfer. This is explicit in the asymptotic form of Eq (29) given in the Appendix B:

$$\frac{1}{\eta_1} = \frac{\phi(R_2^2 - 1)}{2} \left\{ \frac{\phi}{Sh} + \frac{1}{\gamma} \coth[\phi(R_2 - 1)] \right\}, \text{ as } \phi \rightarrow \infty \tag{30}$$

The first and second terms inside the curly brackets in Eq (30) represent the external resistance and internal resistance to mass transfer, respectively. The series-of-resistances nature of Eqs (29) and (30) is a result of using the Robin-type boundary condition, B.C.4, in the evaluation of Eq (17). In both equations the parameters with the greatest influence on the effectiveness factor are: the Thiele modulus, partition coefficient, Sherwood number, and membrane thickness. The influence of the Peclet (Pe_u) number on the effectiveness factor is presented in Appendix A. By definition $\eta = 1$ when the Thiele modulus ϕ becomes zero since this value of the Thiele modulus corresponds with a reaction rate-controlled transfer with no mass transfer limitations.

Zero-order Kinetics. Assuming the zero-order limit, i.e. $K_m \ll c$, the dimensionless form of Eq (2) becomes:

$$\frac{d^2 C_2}{dR^2} + \frac{1}{R} \frac{dC_2}{dR} - \phi_0^2 = 0 \tag{31}$$

Eq (31), subject to B.C. 4 and B.C.5, has a solution of the form:

$$C_2 = \frac{\phi_0^2}{4} \left\{ (R^2 - 1) - 2 \left[R_2^2 \ln R + \frac{\gamma}{Sh} (R_2^2 - 1) \right] \right\} + \gamma C_b \tag{32}$$

The dimensionless zero-order effectiveness factor from Eq (26) is:

$$\eta_0 = - \frac{2}{\phi_0^2(R_2^2 - 1)} \frac{\partial C_2}{\partial R} \Big|_{R=1} = 1 \tag{33}$$

Non-linear Kinetics. The effectiveness factor allows for the determination of the overall reaction rate in terms of the Thiele modulus. However, when the reaction kinetics are not linear as was assumed in the above analysis Eq (26) is not amenable to an analytical solution. A practical measure of evaluating the effectiveness factor is attained by making the following approximation:

$$\frac{dC_2}{dR} \Big|_{R=1} = \frac{C_2|_{R=R_2} - C_2|_{R=1}}{(R_2 - 1)}, \quad (R_2 - 1) \ll 1 \tag{34}$$

Substituting Eq (34) into Eq (26) gives:

$$Y = 1 - \left[C_2|_{R=1} - \frac{\eta\phi_0^2(R_2^2 - 1)(R_2 - 1)}{2(\delta + 1)} \right], \quad (R_2 - 1) \ll 1 \tag{35}$$

where Y is the fractional conversion. Eq (35) allows for empirical determination of the effectiveness factor when the fractional conversion is known, from the following procedure: (i) guess the wall concentration ($C_2|_{R=R_1}$) and obtain the concentration gradient from Eq (34), (ii) substitute the concentration gradient $\frac{dC_2}{dR} \Big|_{R=1}$ into Eq (26) to obtain the effectiveness factor, (iii) substitute the effectiveness factor η into Eq (35) and compare the experimental conversion to the attained value, and (iv) repeat the procedure until the experimental conversion is equal to the value obtained from the iteration.

Results

Fig 2 is a plot of effectiveness factors and corresponding asymptotes, from Eqs (29) and (30) respectively, as functions of the normalized Thiele modulus Φ for different values of the Sherwood number. The normalized modulus is defined as:

$$\Phi = \frac{\phi}{2} (R_2^2 - 1) \tag{36}$$

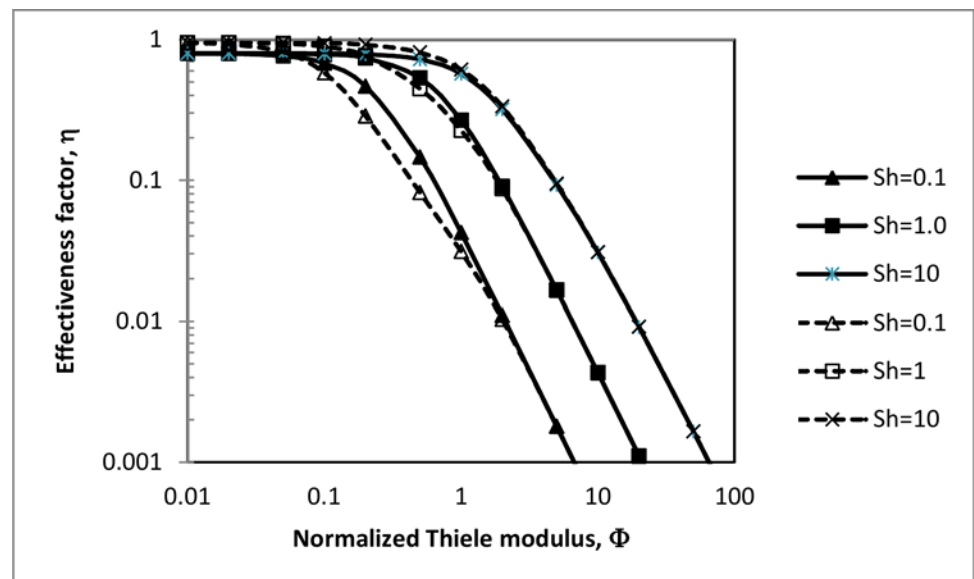


Fig 2. Effectiveness factors (—) from Eq (29) and asymptotes (---) from Eq (30) vs Thiele modulus at different Sherwood numbers.

doi:10.1371/journal.pone.0153000.g002

Eq (30) provides a simple mathematical approximation to Eq (29) and for $\Phi > 1$ gives exact values for the effectiveness factor, as shown in Fig 2. Three regions of Thiele moduli may be defined from Fig 2, as characterised by the effectiveness factor. In the first region ($\Phi < 0.01$) the effectiveness factor is unity, and the rate of solute transport in the MBR is controlled by the rate of reaction. When the MBR is operated in this region the diffusional resistance offered by the membrane is negligible. In the second region ($0.01 < \Phi < 0.1$) the rate of solute transport is limited only by internal diffusion through the membrane, and hence the effectiveness factor is not a function of the Sherwood number. In the third region ($\Phi > 0.1$) external mass transfer limitations control the rate of solute transport through the MBR, and the effectiveness factor is greatly influenced by the Sherwood number. This result is consistent with the Robin-type boundary condition.

Fig 2 may suggest operating the MBR at low values of the Thiele modulus for high effectiveness factors, however substrate conversion at these low values is minimal as can be seen in Fig 3. This figure presents experimental values of conversion and the effectiveness factor for an MBR used for the production of Lignin and Manganese Peroxidases from *Phanerochaete chrysosporium*. The operating parameters of the MBR and kinetic constants of the biofilm are listed in Table 1. From Fig 3 an operating Thiele modulus may be found at which both substrate conversion and the effectiveness factor are optimal. This point corresponds with low effectiveness factors when the objective is to maximise solute conversion [19].

The experimental effectiveness factor in Fig 3 is obtained from Eq (35) and is plotted against the first-order model of Eq (29). The two plots exhibit the same trend, with the model underestimating the effectiveness factor at values of $\Phi < 0.5$. This is because at low values of the Thiele modulus solute transport is reaction rate controlled and the first-order kinetics premise assumes a lower rate of reaction than the maximum. At higher values of the Thiele modulus solute transport is limited by internal and external diffusion, and the first-order model approximately matches the experimental effectiveness factor.

In the region of internal diffusional limitation ($0.01 < \Phi < 0.1$) radial convective flows can significantly improve the effectiveness factor, as illustrated in Fig 4. In this figure the relative increases in the effectiveness factor ($\eta/\eta_{Pe=0}$) are plotted against normalised Thiele moduli for

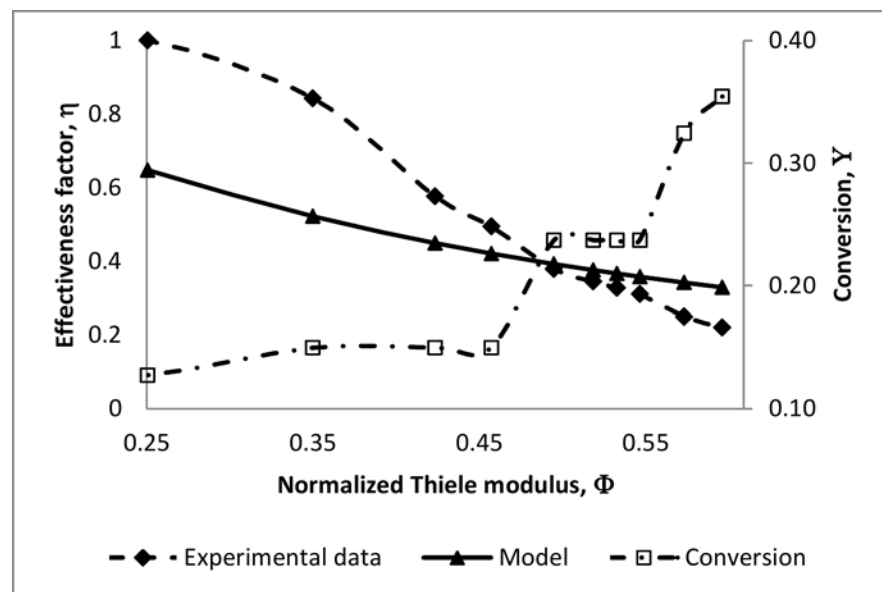


Fig 3. Effectiveness factor and glucose conversion vs normalized Thiele modulus (Sh = 0.83).

doi:10.1371/journal.pone.0153000.g003

Table 1. Parameter values used to determine the effectiveness factor in Fig 3 [25].

Model parameter	Symbol	Unit	Basic measured value
Membrane inner radius	R_1	m	6.98×10^{-4}
Membrane outer radius	R_2	m	9.63×10^{-4}
Effective membrane length	L	m	0.230
Lumen-side entrance velocity	u_0	ms^{-1}	3.04×10^{-4}
Permeation velocity	v_0	m s^{-1}	8.82×10^{-6}
Glucose diffusivity	D_{AB}	$\text{m}^2 \text{s}$	1.59×10^{-9}
Glucose inlet concentration	c_0	g dm^{-3}	10.00
Maximum specific growth rate	μ_{max}	h^{-1}	0.035
Saturation constant	K_m	g dm^{-3}	9.350
Yield of biofilm per substrate	$Y_{x/s}$	g/g	0.202

doi:10.1371/journal.pone.0153000.t001

different values of the radial Peclet number. The effectiveness factors in Fig 4 are obtained from Eq (A8) in Appendix A. The increase in η with Pe_v , is only restricted to the region of internal diffusional limitation. The maximum relative increase in the effectiveness factor is obtained in the transitional region from kinetic to internal-diffusional control ($\Phi \approx 0.01$), and minimal in the boundary region between internal-diffusional control and external mass transfer limitation. Increasing Pe_v , outside this region may drastically reduce the contact time between the substrate and the biocatalyst, and hence lead to reduced substrate conversions as was shown by Calabro *et al.* [17]. In this region ($\Phi > 0.1$), as previously discussed the effectiveness factor can be improved by increased Sherwood numbers.

Conclusion

Mathematical models were developed for solute concentration profiles and effectiveness factors in an MBR, assuming the zero-order and first-order limits of the Michaelis-Menten (or Monod) equation. The first-order kinetic model was shown to be applicable only when the MBR is operated at high Thiele moduli. Experimental results show that the effectiveness factor

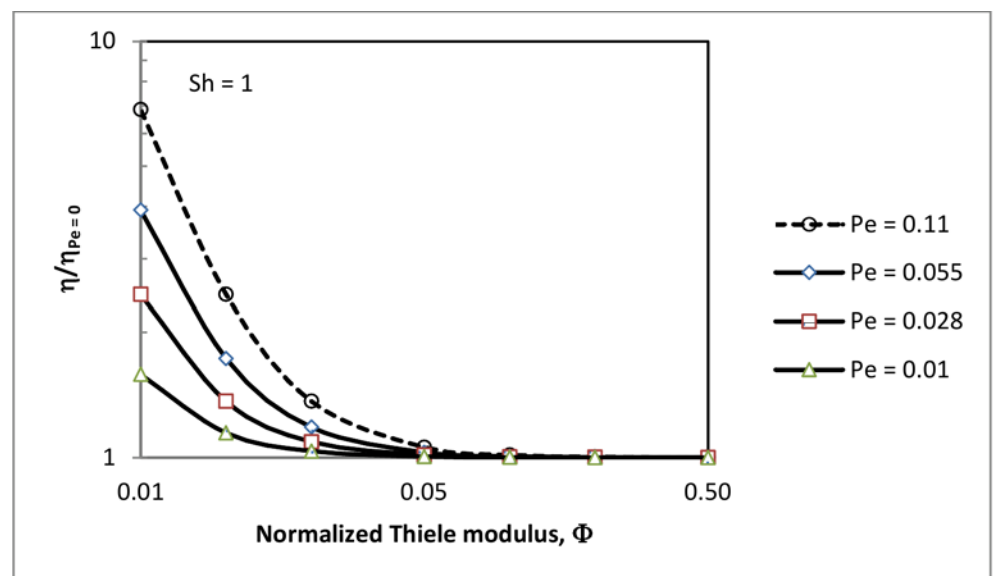


Fig 4. Relative increase in effectiveness factor vs normalized Thiele modulus at different Peclet numbers.

doi:10.1371/journal.pone.0153000.g004

decreases with increasing Thiele modulus, while the fractional conversion increases with an increase in this parameter. The developed model allows for the determination of the operating point at which both the conversion and effectiveness factor are optimal. It was also shown that the radial Peclet number can significantly improve the performance of an MBR operating under internal diffusional limitations.

Appendix A

First-order perturbation approximation of the effectiveness factor

The solution of Eq (15) may be approximated by an asymptotic expansion:

$$C_2 = C_2^{(0)} + \kappa C_2^{(1)} + \kappa^2 C_2^{(2)} + \dots + \kappa^n C_2^{(n)} \tag{A1}$$

The zero-order approximation $C_2^{(0)}$ was given in Section 2.3 as:

$$C_2^{(0)} = B_1 I_0(\phi R) + B_2 K_0(\phi R) \tag{A2}$$

The first-order approximation $C_2^{(1)}$ is a solution of the equation:

$$\frac{d^2 C_2^{(1)}}{dR^2} + \frac{1}{R} \frac{dC_2^{(1)}}{dR} + \phi^2 C_2^{(1)} = 2Pe_u \beta \left[R \left(1 - \frac{R^2}{2} \right) \right] \frac{dC_2^{(0)}}{dR} \tag{A3}$$

The modified Bessel function $K_\nu(x)$ tends to zero as $|x| \rightarrow \infty$ for all values of ν . The contribution of this function in Eq (A3) is therefore only significant as $x \rightarrow 0$. In this region the limiting form of $K_\nu(x)$ is [23]:

$$K_\nu(x) \sim \frac{1}{2} \Gamma(\nu) \left(\frac{1}{2} x \right)^{-\nu} \quad (\nu > 0) \tag{A4}$$

where $\Gamma(n)$ is the Gamma function. The solution of Eq (A3) follows the same procedure as Godongwana *et al.* [13], and is of the form:

$$C_2^{(1)} = \frac{Pe_u \beta \kappa}{\phi^2} \left\{ \frac{3\sqrt{\pi} B_1}{2} \left[\frac{(\phi R)^2 I_2(\phi R)}{2^2 \Gamma(2\frac{1}{2})} + \alpha_1 \frac{(\phi R)^3 I_3(\phi R)}{2^3 \Gamma(3\frac{1}{2})} + \alpha_2 \frac{(\phi R)^4 I_4(\phi R)}{2^4 \Gamma(4\frac{1}{2})} \right] - \frac{B_2}{\phi^2} [(\phi R)^2 - 2\phi^2 + 4] \right\} \tag{A5}$$

where

$$\alpha_1 = -\frac{20}{3\phi^2}, \quad \text{and} \quad \alpha_2 = -\frac{35}{4\phi^2} \tag{A6}$$

The effectiveness factor is obtained by substituting the derivatives of Eqs (A2) and (A5) into Eq (28), making use of the following property of Bessel functions [23]:

$$\left(\frac{1}{z} \frac{d}{dz} \right)^k \{ z^\nu I_\nu(z) \} = z^{\nu-k} I_{\nu-k}(z) \tag{A7}$$

This gives:

$$\eta = \frac{2\gamma [K_1(\phi) \cdot I_1(\phi R_2) - I_1(\phi) \cdot K_1(\phi R_2) - \xi]}{\phi(R_2^2 - 1) \{ [K_0(\phi) \cdot I_1(\phi R_2) + I_0(\phi) \cdot K_1(\phi R_2)] + \psi \}} \tag{A8}$$

where

$$\zeta = Pe_u \beta \kappa \left\{ \frac{3\sqrt{\pi} \cdot K_1(\phi R_2)}{8} \left[\frac{I_1(\phi)}{\Gamma(2\frac{1}{2})} + \alpha_1 \frac{\phi I_2(\phi)}{2\Gamma(3\frac{1}{2})} + \alpha_2 \frac{\phi^2 I_3(\phi)}{4\Gamma(4\frac{1}{2})} \right] - \frac{2I_1(\phi R_2)}{\phi^3} \right\} \quad (A9)$$

Appendix B

Asymptotic solution of the Effectiveness factor ($\phi \rightarrow \infty$)

Eq (17) may be written as:

$$\frac{\epsilon^2}{R} \frac{d}{dR} \left(R \frac{dC_2}{dR} \right) - C_2 = 0 \quad (B1)$$

where:

$$\epsilon = \frac{1}{\phi} \quad (B2)$$

The solution of Eq (17) may be approximated by an asymptotic expansion when $\epsilon \ll 1$ as:

$$C_2 = b_0 + \epsilon b_1 + \epsilon^2 b_2 + \dots \quad (B3)$$

In order to keep the second-order derivative in the solution of the coefficient b_0 in Eq (B3), the following variable is defined:

$$\omega = \frac{1 - R}{\epsilon} \quad (B4)$$

Eq (B1) then becomes:

$$\frac{d^2 C_2}{d\omega^2} - \frac{\epsilon}{(1 - \epsilon\omega)} \frac{dC_2}{d\omega} - C_2 = 0 \quad (B5)$$

The leading order term sub-problem is:

$$\frac{d^2 b_0}{d\omega^2} - b_0 = 0 \quad (B6)$$

The corresponding boundary conditions are B.C.4 and B.C.5 of Eq (3):

$$\frac{db_0}{d\omega} \Big|_{\omega=0} = \epsilon Sh \left[C_b - \frac{b_0(0)}{\gamma} \right] \quad (B7a)$$

and

$$\frac{db_0}{d\omega} \Big|_{\omega=(1-R_2)/\epsilon} = 0 \quad (B7b)$$

The solution of Eq (B6), subject to the boundary conditions of Eq (B7) is:

$$b_0 = \Lambda_1 e^\omega + \Lambda_2 e^{-\omega} \quad (B8)$$

where

$$\Lambda_1 = \frac{1}{\phi \left(1 + \frac{Sh}{\phi\gamma} \right)} \left\{ \frac{\left(1 - \frac{Sh}{\phi\gamma} \right) Sh C_b e^{-[\phi(R_2-1)]}}{\sinh[\phi(R_2-1)] + \frac{Sh}{\phi\gamma} \cosh[\phi(R_2-1)]} + Sh C_b \right\} \quad (B9)$$

And

$$\Lambda_2 = \frac{1}{\phi} \left\{ \frac{ShC_b e^{-[\phi(R_2-1)]}}{\sinh[\phi(R_2-1)] + \frac{Sh}{\phi} \cosh[\phi(R_2-1)]} \right\} \quad (B10)$$

The effectiveness factor is obtained by taking the derivative of Eq (B8) and substituting into Eq (28) to obtain:

$$\frac{1}{\eta_1} = \frac{\phi(R_2^2 - 1)}{2} \left\{ \frac{\phi}{Sh} + \frac{1}{\gamma} \coth[\phi(R_2 - 1)] \right\} \quad (B11)$$

Acknowledgments

The author would like to thank the National Research Foundation (RSA) for supporting this work. Special thanks to Dr S.K. Ntwampe and Dr M.S. Sheldon for making available the data used in Fig 3.

Author Contributions

Conceived and designed the experiments: BG. Performed the experiments: BG. Analyzed the data: BG. Contributed reagents/materials/analysis tools: BG. Wrote the paper: BG.

References

1. Chang HN, Furusaki S. Membrane bioreactors: present and prospects. *Adv Biochem Eng Biotechnol.* 1991; 44:27–64. PMID: [1781318](#)
2. Giorno L, Drioli E. Biocatalytic membrane reactors: applications and perspectives. *Tibtech.* 2000; 18:339–49.
3. Charcosset C. Membrane processes in biotechnology: an overview. *Biotechnol Adv.* 2006; 24(5):482–92. PMID: [16687233](#)
4. Curcio S, Calabro V, Iorio G. A theoretical and experimental analysis of a membrane bioreactor performance in recycle configuration. *J Memb Sci.* 2006; 273(1–2):129–42.
5. Nagy E. Basic equations of the mass transport through a membrane layer. Boston: Elsevier; 2012.
6. Aris R. The mathematical theory of diffusion and reaction in permeable catalysts. Volume 1, the theory of the steady state. Oxford: Clarendon Press; 1975.
7. Webster IA, Shuler ML. Mathematical models for hollow-Fiber enzyme reactors. 1978;20:1541–56.
8. Webster IA, Shuler ML, Rony PR. Whole-cell hollow-fiber reactor: effectiveness factors. 1979;21:1725–48.
9. Willaert R, Smets A, Vuyst L De. Mass transfer limitations in diffusion-limited isotropic hollow fiber bioreactors. *Biotechnol Tech.* 1999; 13(7):317–23.
10. Waterland LR, Michaelis AS, Robertson CR. A theoretical model for enzymatic catalysis using asymmetric hollow fiber membranes. *Am Inst Chem Eng J.* 1974; 20(1):50–9.
11. Ye H, Das DB, Triffitt JT, Cui Z. Modelling nutrient transport in hollow fibre membrane bioreactors for growing three-dimensional bone tissue. *J Memb Sci.* 2006; 272:169–78.
12. Jayaraman VK. The solution of hollow fiber bioreactor design equations. *Biotechnol Prog.* 1992; 8(5):462–4. PMID: [1369227](#)
13. Godongwana B, Solomons D, Sheldon MS. A solution of the convective-diffusion equation for solute mass transfer inside a capillary membrane bioreactor. *Int J Chem Eng.* 2010; 2010:1–12.
14. Dall-Bauman L, Ilias S, Govind R. Analysis of hollow fiber bioreactor wastewater treatment. *Biotechnol Bioeng.* 1990; 35:837–42. PMID: [18592585](#)
15. Tanyolac A, Beyenal H. Effectiveness factor for a hollow-fiber biofilm reactor at maximum substrate consumption. *Chem Eng J.* 1996; 62:149–54.
16. Jayaraman VK, Kulkarni BD. An efficient algorithm for solving hollow-fiber bioreactor design equations. *Chem Eng J Biochem Eng J.* 1997; 65(1):77–80.

17. Calabrò V, Curcio S, Iorio G. A theoretical analysis of transport phenomena in a hollow fiber membrane bioreactor with immobilized biocatalyst. *J Memb Sci*. 2002; 206(1–2):217–41.
18. Gonzo EE, Gottifredi JC. A simple and accurate method for simulation of hollow fiber biocatalyst membrane reactors. *Biochem Eng J*. 2007; 37:80–5.
19. Nagy E, Dudás J, Mazzei R, Drioli E, Giorno L. Description of the diffusive–convective mass transport in a hollow- fiber biphasic biocatalytic membrane reactor. *J Memb Sci*. 2015; 482:144–57.
20. Godongwana B, Solomons D, Sheldon MS. A finite-difference solution of solute transport through a membrane bioreactor. *Math Probl Eng*. 2015; 2015:1–8.
21. Lewandowski Z, Beyenal H. *Fundamentals of biofilm research*. Boca Raton: CRC Press; 2007.
22. Wickramasinghe SR, Garcia JD, Han B. Mass and momentum transfer in hollow fibre blood oxygenators. *J Memb Sci*. 2002; 208:247–56.
23. Abramowitz M, Stegun IA. *Handbook of mathematical functions*. New York: Dover; 1965.
24. Lieb T, Pereira C. Reaction kinetics. In: Green W, Perry R, editors. *Perry's chemical engineering handbook*. 8th ed. New York: McGraw-Hill; 2007.
25. Ntwampe SKO, Sheldon MS. Quantifying growth kinetics of *Phanerochaete chrysosporium* immobilised on a vertically orientated polysulphone capillary membrane: Biofilm development and substrate consumption. *Biochem Eng J*. 2006; 30(2):147–51.